

Crustal and Uppermost Mantle Structures beneath the Qattara Depression Area from the Transfer and Receiver Functions method

Ali Gharib, Ahmed Hosny, Imam Marzouk, Saud Abdselehady; Mona Hegazi; Gad Alkareem Mohamed; Iman Farag, Ramadan Bakir, Mona Mohamed, Hazem Badreldin and Samar Gharib

Seismology Department, National Research Institute of Astronomy and Geophysics (NRIAG), Egypt.

ahhosny2000@yahoo.com

Abstract: The aim of this study is to investigate the crustal and upper mantle structure beneath and around the Qattara Depression area using the Transfer (TF), the Receiver Function (RFs), and the joint inversion tool. Tele and regional seismic data recorded by the Egyptian National seismic network (ENSN) were collected for implementing our proposed study. Results obtained by the TF tool are correlated with those obtained by the RFs tool. The results detected a thin layer near the surface with 2.3 km thick and V_p of 3.5 km/sec, underlain by a thick layer up to 6.8 km with V_p of 4.87 km/sec. Those two layers represent the upper crust, while the middle crust is shown by a thick layer of 7.0 km with V_p of 6.1 km/sec, and the lower crust is represented by a thicker layer (14.4 km) with moderate V_p of 6.9 km/sec underlain by an upper mantle layer with V_p of about 8.2 km/sec. The obtained results of RFs revealed that the crustal thickness beneath the Sallum (SLM) and Dabaa (DB2) site is about 32 km, while it is 35 km beneath the Siwa and Frafra Oasis areas. Due to the thick sedimentary column with surficial soft sediment saturated with hot ground water, the average V_p/V_s ratio that observed beneath these areas was high value of 1.9. Based on the Joint inversion results in regards to the Moho discontinuity, depths are consistent with that obtained from the stacking of the receiver functions. Moho depths are detected at shear wave velocity of 4.3 km/s. A low velocity zone is observed at the surface layer beneath the study area and increasing with depth. Gradational and sharp Moho interfaces are obtained beneath our study area. An average velocity model is derived for locating local and regional earthquakes occur in and around the Qattara region. In comparison with other previous studies concerning the crustal structure of northern Egypt and conducted on the same study area, our results are found to be in good agreement with these previous works.

[Ali Gharib, Ahmed Hosny, Imam Marzouk, Saud Abdselehady; Gad Alkareem Mohamed; Iman Farag, Ramadan Bakir, Mona Mohamed, Hazem Badreldin and Samar Gharib. **Crustal and Uppermost Mantle Structures beneath the Qattara Depression Area from the Transfer and Receiver Functions method.** *J Am Sci* 2016;12(4):1-13]. ISSN 1545-1003 (print); ISSN 2375-7264 (online). <http://www.jofamericanscience.org>. 1. doi:[10.7537/marsjas12041601](https://doi.org/10.7537/marsjas12041601).

Key words: crustal structures, velocity model, north of Egypt.

1. Introduction

As a part of the research project supported by the STDF (project No. 5314), the crustal structure of the Qattara depression, located in northern west of Egypt as labeled as region 4 in figure (1), is investigated. The Transfer (TF) and Receiver Functions (RF) tools have been applied for the seismic data obtained from the broadband (BB) and 3- components short period (SP) seismic stations of the Egyptian National Seismic Network (ENSN). This is to investigate the seismic discontinuities in the crust down to the upper mantle beneath the ENSN station sites. The Crustal structure beneath 9 seismic stations (BB & SP) sites around the Qattara

Depression area (figure 2) is derived using P-wave amplitude ratios from selected regional and teleseismic earthquakes. About 200 earthquakes from different azimuths are selected so as to cover the area around Qattara area. The records of the North Western seismic stations of ENSN are used during the period from 2008 to 2014.

However, crustal model are derived for each station site individually and by correlating the nearby station site models to obtain the general model beneath the Qattara Depression area.

Tectonics of the Qattara Depression area:

The study area is a part of the North Western desert region; it is characterized by almost featureless plain surface, which is cut by the Qattara Depression. The recent seismological history reveals that this region shows a very low seismic activity, this explains the absence or rareness of the surface faults. This indicates also that the recent tectonics of the study area is more stable than other adjacent areas close to the Mediterranean Sea or Nile-Delta. The dominant Pre-Tertiary structural style of the Western desert of Egypt and Sirte basin is normal faulting, essentially a horset-graben structure (Sestini, 1984).

There is no active deformation west of the Delta (SOFRATOM Group, 1984), in particular there is no faulting along Wadi El-Natroun Depression, sand bars between Wadi El-Natroun Al- Dabbaa and south of El-

Dabbaa, including the Qattara depression. This indicates that all the activity between Qattara, Al-Dabbaa platform and adjacent regions of the east

appear to be taken up by faults under the Nile Delta within the Suez-Alexandria Fault zone.

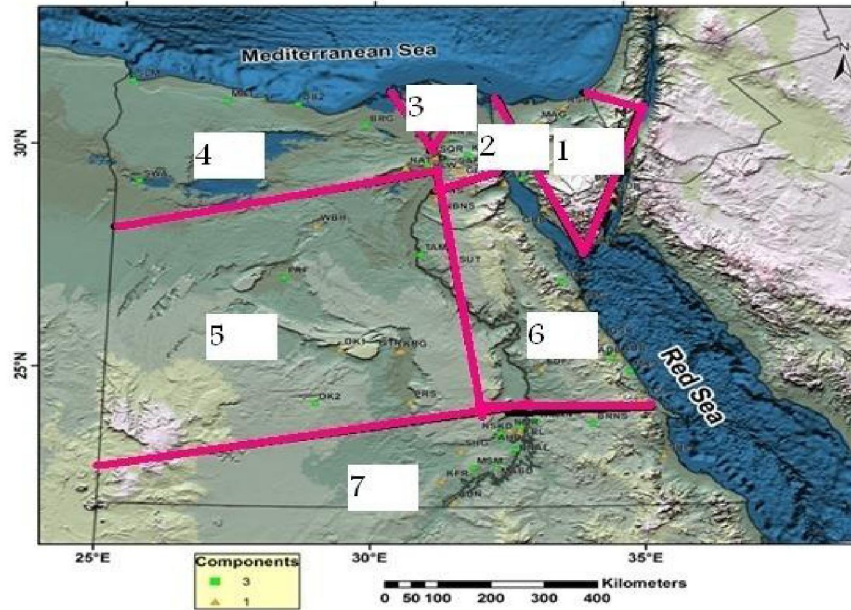


Fig. (1) Topographic map showing the seven regions of STDF project No. 5314, the Qattara depression is labelled as area (4).

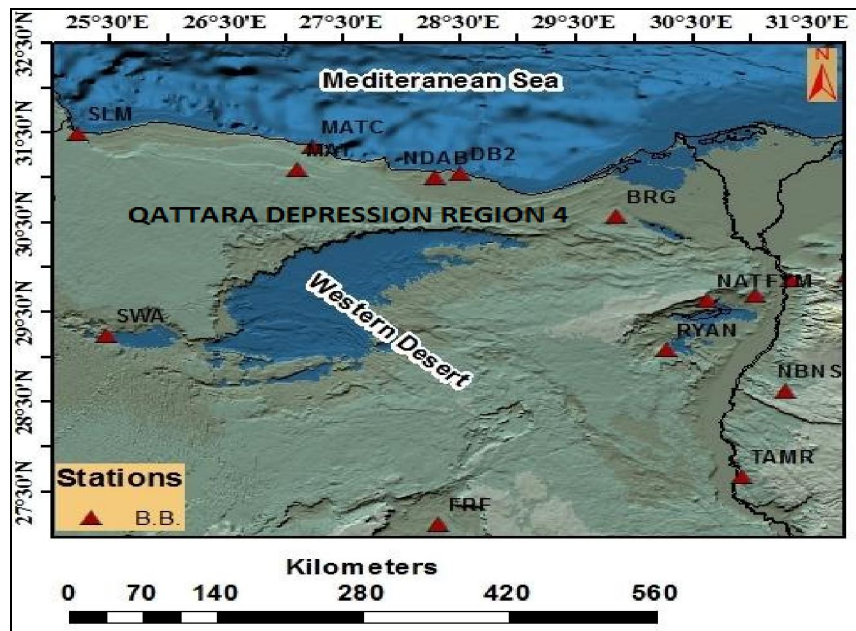


Fig. 2 location map of the seismic stations in and around the Qattara depression (area 4).

Previously, the Gravity, magnetic and seismic data (Figure 3) was used to delineate the Seismotectonic settings of the Northern Egypt (Gamal, 2013). The most important event, that reached this zone, was on September 12, 1955 with ML 6.6 and maximum intensity $I_0 = IX$, Maamoun et al, (1979) as

indicated in figure (4). While the seismic activity within the Western Desert shows some scattered events which may be related to the shelf break, the transition from continental to oceanic crusts and/or some tectonically deep-seated active faults.

The refined results for the seismic velocity structure for the Arabian Platform suggested that, the crust consists of four distinct layers. The upper crustal layer has a V_p of about 5.43 km/sec and is about 2.4 km thick. The second layer (middle crust) has a velocity of about 6.42 km/sec and 8 km thick. The third layer (lower crust) shows a velocity of 7.0 km/sec and

12km thick. The lower crustal layer has a velocity of about 7.78 km/sec and 18km thick. The Mohorovicic discontinuity beneath the north Western Desert varies from 30 km depth in the NE and SE with 8.2 km/sec mantle velocity to 40 km depth in the NW and SW with 8.1 km/sec mantle velocity, Gamal, 2013.

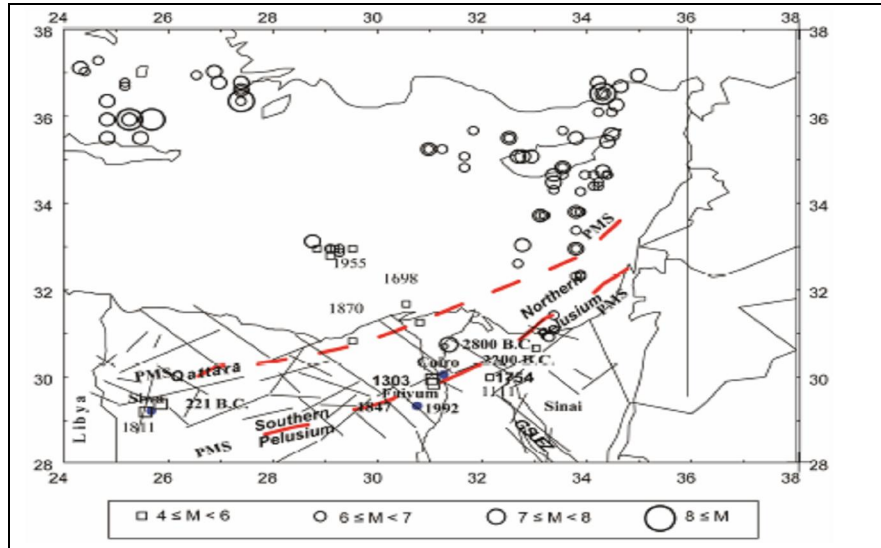


Fig. 3: Seismicity and main tectonic features of Northern Egypt (after Gamal, 2013).

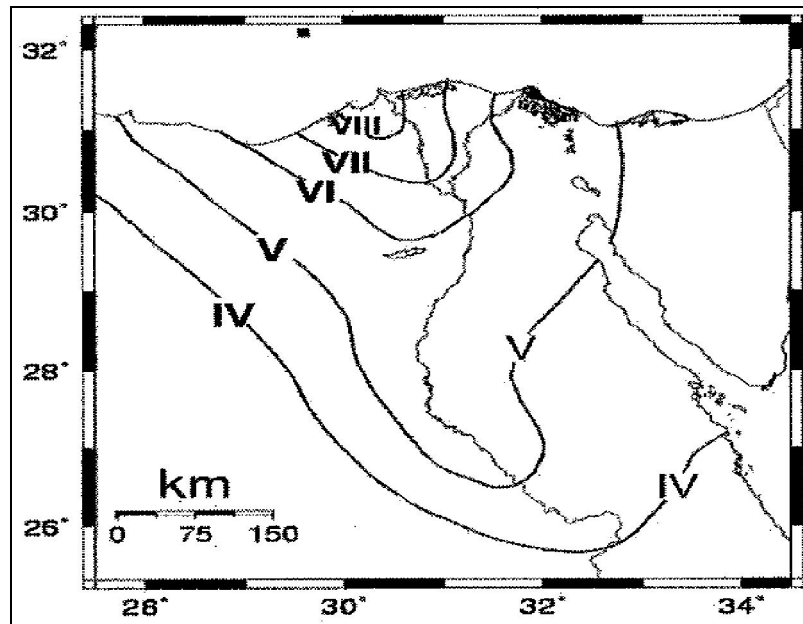


Figure (4): Isoseismal map of Sept. 1955 earthquake (Maamoun et al, 1979)

Methodologies and results

Generally, three different techniques were used for implementing the current study, the transfer function, the stacking of the receiver functions, and the joint inversion of the receiver functions and the group velocity dispersion, as the following:

A-Transfer function method (TF)

The basic mathematical background of this tool is given in detail by Al-Amri and Gharib 2000, Gharib 2005 and Hijazi 2007 which is based upon Thomson-Haskell matrix formulation (Thomson 1950 and Haskell 1953). To get a clear idea about the algebraic

solution of the method see, Haskell, 1953, 1962; Phinney, 1964 and Fernandez, 1965. This method is depended on the assumptions that, the layered media have to be horizontal, homogeneous and isotropic. The velocity and density are linearly changed with depth, while the Poisson's ratio is supposed to be equal to 0.25. The spectral ratios method is based on the technique, which requires only 3-components seismograms of the single station to constrain the crustal model beneath the seismic station. However, the obtained solution is not unique due to the theoretical assumption in Thomson–Haskell formulation and the complexity of the earth's crust. The physical characteristics of the crustal and upper mantle structure, were obtained on the basis of P-wave spectra. In order to obtain the energy of the source, the observed spectra of the vertical components of motion are divided by the spectra of the two rotated horizontal components (Radial and Transverse). The ratios of the P-wave spectra provide the observed crustal transfer function, which depends on the system of layers under the recording seismic station.

B- Receiver functions method (RFs)

Receiver functions are a time series that show the response of Earth's structure beneath the recording station and are commonly used for investigating crustal structure (Langston, 1979). The direct P wave, the P-to-S conversion at the Moho (Ps) and its reverberations between the Moho and the free surface (PpPs and

PsPs+PpSs) are the main phases of the waveform. The thickness of the crust and Poisson's ratio beneath a seismic station can be determined using the arrival time difference between the direct and the converted phases (Langston, 1979; Ligorria and Ammon, 1999; Zandt and Ammon, 1995; Zhu and Kanamori, 2000).

C- H-k stacking method

The H-k stacking method of Zhu and Kanamori (2000) was applied to the receiver functions for estimating the crustal thickness and V_p/V_s ratio beneath each seismic station. This method reduces the ambiguity in Moho depth (H) and V_p/V_s (κ) estimates by incorporating the later multiple converted phases from the Moho (PpPs and PsPs+PpSs). In this method, the receiver functions are transformed to the H- κ parameter space by an objective function:

$$S(H, \kappa) = \sum_{j=1}^N w_j r_j(t_1) + w_2 r_j(t_2) - w_3 r_j(t_3) \dots \dots (1)$$

Where t_j are the travel times of the three main P-to-S converted phases from the Moho (Ps, PpPs and PsPs+PpSs), w_i are weights assigned to each phase (sum of $w_i = 1$), r_j is the receiver function amplitude for the j-th receiver function and N is the number of receiver functions. S(H, κ) reaches its maximum when optimal values for H and κ are determined, satisfying a simple layer over a half space crustal model.

Table (1): The initial crustal model which is used as a starting model (after Marzouk 1988).

Layers		Depth Km	VP Km/sec	VS Km/sec	Density Gm/cm ³
Upper crust	Superficial	00	3.5	1.977	2.2
	Weathered rock	0.5	5.8	3.258	2.3
Middle Crust		14.5	6.2	3.45	2.6
Lower crust		20.5	6.9	3.87	2.9
Upper Mantle		36.5	8.1	4.6	3.1

Structural models obtained from the transfer function (TF) Tool

Beneath each seismic station at the study region, using the transfer function the P-wave velocity, shear

wave velocity, and density at different depths are provided, as listed in bellow.

Table (2): Structural model beneath DB2 (SP) station site, cross-correlation Coefficient = 96%.

Layers		Depth Km	VP Km/sec	VS Km/sec	Density Gm/cm ³
Upper crust	Superficial	00	3.2	1.82	2.1
	Weathered rock	1.78	4.1	2.34	2.3
Middle Crust		10.1	4.99	2.8	2.5
Lower crust		14.54	6.6	3.77	2.9
Upper Mantle		27.98	8.1	4.6	3.3

Table (3): Structural model beneath BRG station site, cross-correlation Coefficient =92%.

Layers	Depth KM	VP Km/sec	VS Km/sec	Density Gm/cm ³
Super-facial	00.0	4.04	2.39	2.1
Upper crust	2.5	6.32	3.67	2.3
Lower crust	11.0	7.59	4.41	2.5
Upper Mantle	29.6	8.1	4.7	2.9

Table (4): Structural model beneath MAT station site, cross-correlation Coefficient = 95%.

Layers	Depth KM	VP Km/sec	VS Km/sec	Density Gm/cm ³	
Upper crust	Superficial	00	3.5	2	2.1
	Weathered rock	2.07	4.6	2.6	2.3
Middle Crust	8.21	5.6	3.2	2.5	
Lower crust	15.71	6.7	3.83	2.9	
Upper Mantle	30.71	8.1	4.6	3.3	

Table (5): Structural model beneath KOT station site, cross-correlation coefficient = 96%.

Layers	Depth KM	VP Km/sec	VS Km/sec	Density Gm/cm ³	
Upper crust	Superficial	00	3.9	1.65	2.1
	Weathered rock	2.9	5.83	3.533	2.3
MIDDLE CRUST	8.3	6.73	3.84	2.5	
Lower crust	19.3	7.23	4.13	2.9	
Upper Mantle	33.8	8.2	4.68	3.3	

Table (6): Structural model beneath ANS station site, the cross-correlation Coefficient = 88%.

Layers	Depth KM	VP Km/sec	VS Km/sec	Density Gm/cm ³	
Upper crust	Superficial	00	3.5	2	2.1
	Weathered rock	2.07	4.6	2.6	2.3
MIDDLE CRUST	8.21	5.6	3.2	2.5	
Lower crust	15.71	6.7	3.83	2.9	
Upper Mantle	30.71	8.1	4.6	3.3	

Table (7): Structural model beneath SWA station site, cross-correlation Coefficient = 91%.

Layers	DEPTH KM	VP Km/sec	VS Km/sec	Density Gm/cm ³	
Upper crust	Superficial	00	3.55	2.03	2.1
	Weathered rock	2	5	2.89	2.3
Middle Crust	7	6.11	3.49	2.5	
Lower crust	14.5	6.7	3.85	2.9	
Upper Mantle	32.28	8.1	4.6	3.3	

Table (8): Structural model beneath NAT station site, cross-correlation Coefficient = 99%.

Earth Layers	Depth Km	VP Km/sec	VS Km/sec	Density Gm/cm ³	
Upper crust	Superficial	00	3.45	1.97	2.1
	Weathered rock	2.54	4.78	2.73	2.3
Middle Crust	9.77	6.7	3.85	2.5	
Lower Crust	16.54	7.1	4.06	2.9	
Upper Mantle	32.77	8.1	4.6	3.3	

Table (9): Structural model beneath DB2 (BB) station site, cross-correlation Coefficient = 93%.

Earth Layers		Depth Km	VP Km/sec	VS Km/sec	Density Gm/cm ³
Upper crust	Superficial (Soft sediment)	00	3.2	1.82	2.1
	Weathered rock(Hard sediment)	1.78	4.1	2.34	2.3
Middle Crust		10.1	4.99	2.8	2.5
Lower Crust		14.54	6.8	3.8	2.9
Upper Mantle		27.98	8.1	4.6	3.3

Table (10): Structural model beneath FYM station site, cross-correlation Coefficient = 96%.

Earth Layers		Depth Km	VP Km/sec	VS Km/sec	Density Gm/cm ³
Upper crust	Superficial	00	3.9		2.1
	Weathered rock	2.9	5.85		2.3
Middle Crust		8.3	6.73		2.5
Lower Crust		19.3	7.23		2.9
Upper Mantle		33.8	8.3		3.3

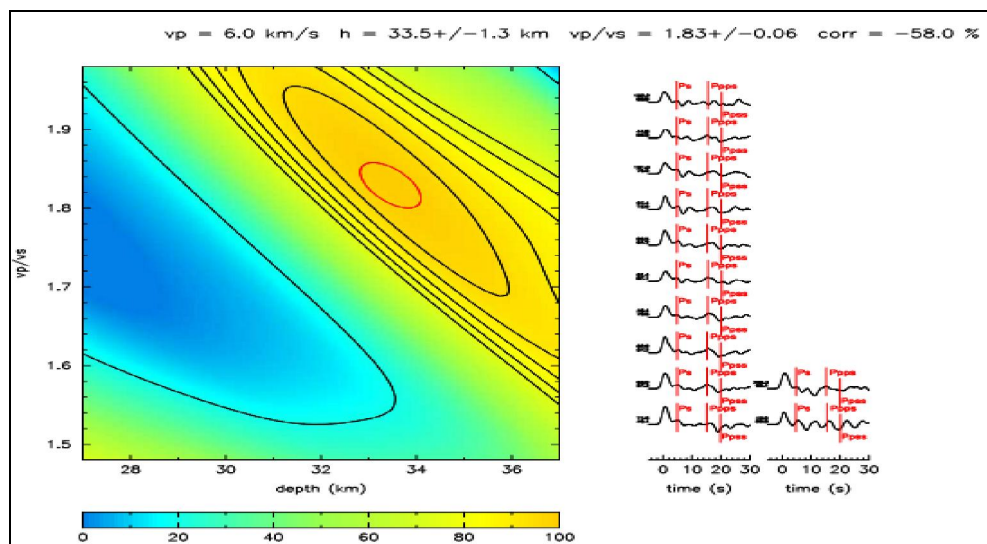
D- Joint inversion of the receiver functions and group velocity dispersion

Using the method of Juliá et al., (2000, 2003), the shear wave velocity structure of the crust beneath each seismic station can be obtained by jointly inverting receiver functions and Rayleigh wave group velocity measurements. This method employs a linearized damped least squares inversion that incorporates a priori smoothness and influence constraints. A combination of surface wave dispersion curves and receiver functions provides constraints on the shear wave velocity of the propagation medium that improve those provided by either of the data sets considered separately, and helps to avoid over interpretation of single data sets (Ozalaybey et al., 1997; Juliá et al., 2000, 2003, 2005; Dugda et al., 2007).

Results from the receiver functions

Beneath each seismic station at the study area, by stacking of the obtained RFs, the crustal thickness and the Vp/Vs ratio have been derived obtained, as detailed in below:

Beneath the first area, station SLM, at Sallum area the crustal thickness is measured at ~ 32 km and the average Vp/Vs ratio is 1.8, as shown in figure (5). While, beneath the second station located at El-Dabaa area, (DB2 station) the crustal thickness was measured at 33.0 and the average Vp/Vs ratio is 1.96, which consider high value due to the seepage of the Sea water through the transverse faults cut El-Dabaa area. Result of DB2 station is shown in figure (6).

**Figure (5): $H-\kappa$ (H —crustal thickness; κ —Vp/Vs) stack of the receiver function for station SLM.**

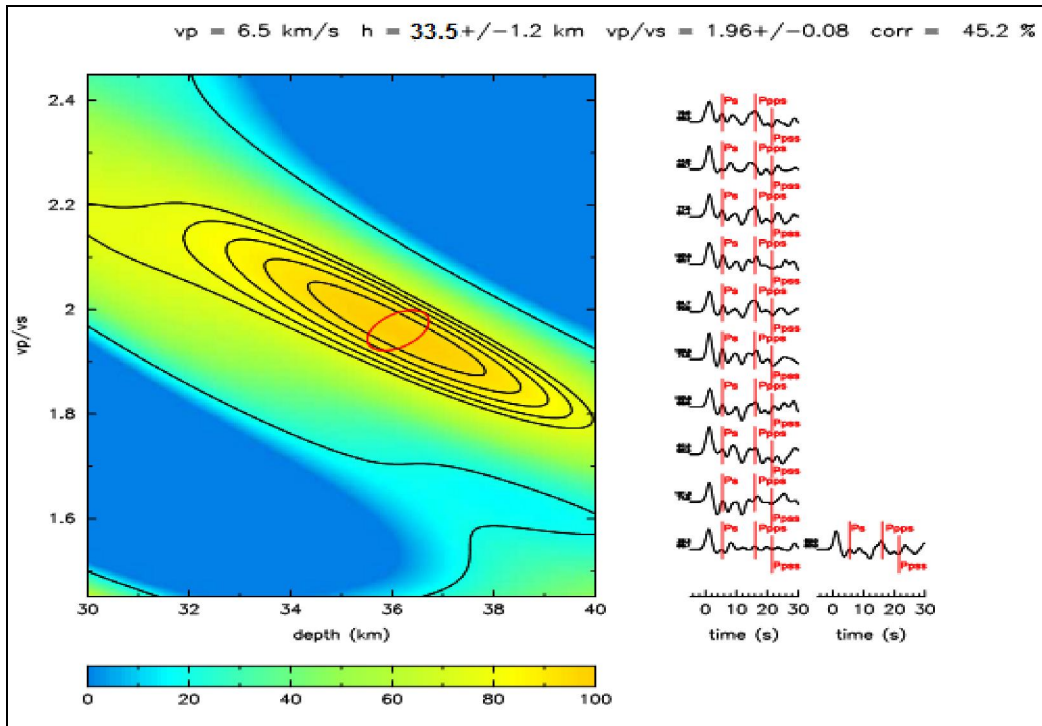


Figure (6) H - κ (H —crustal thickness; κ — V_p/V_s) stack of the receiver function for DB2 station.

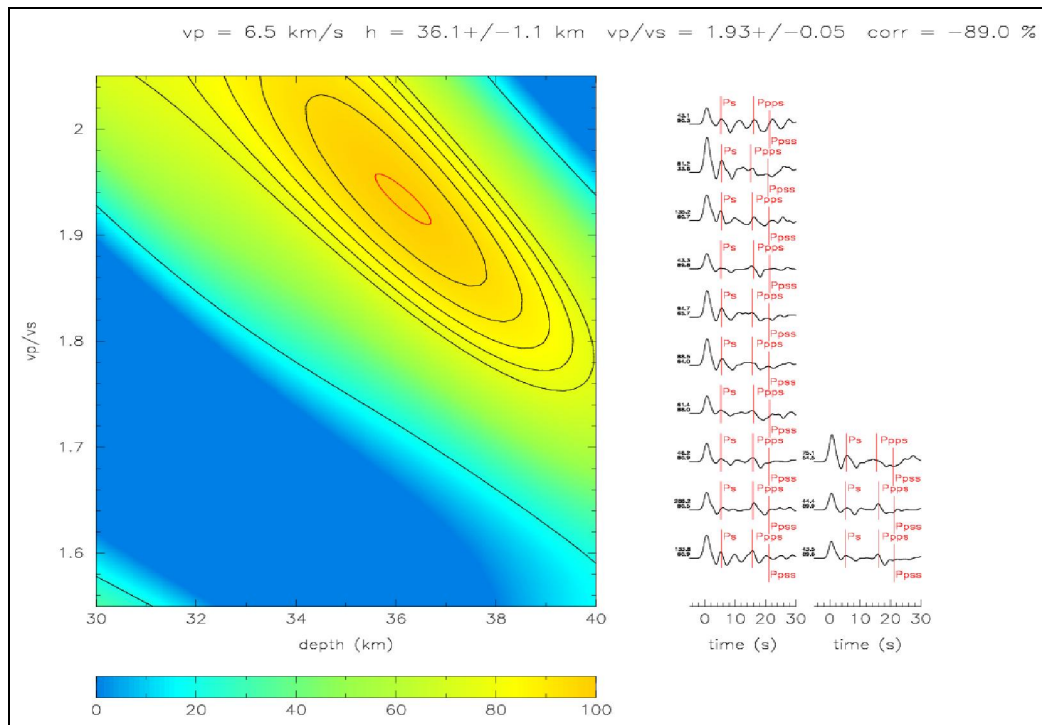


Figure (7) H - κ (H —crustal thickness; κ — V_p/V_s) stack of the receiver function for SWA station.

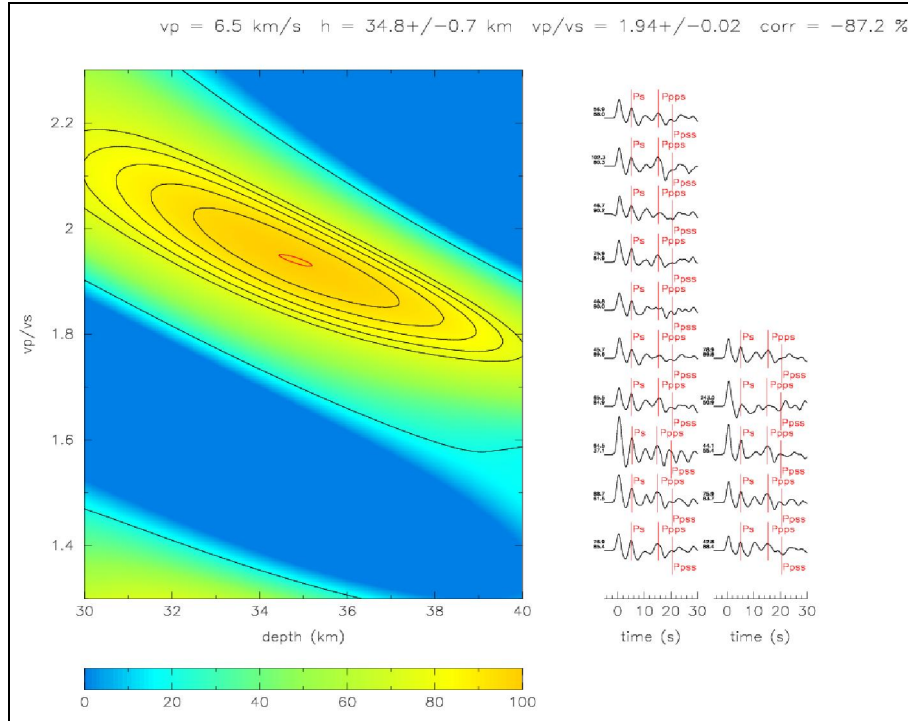


Figure (8): $H-\kappa$ (H —crustal thickness; κ — V_p/V_s) stack of the receiver function for FRF station.

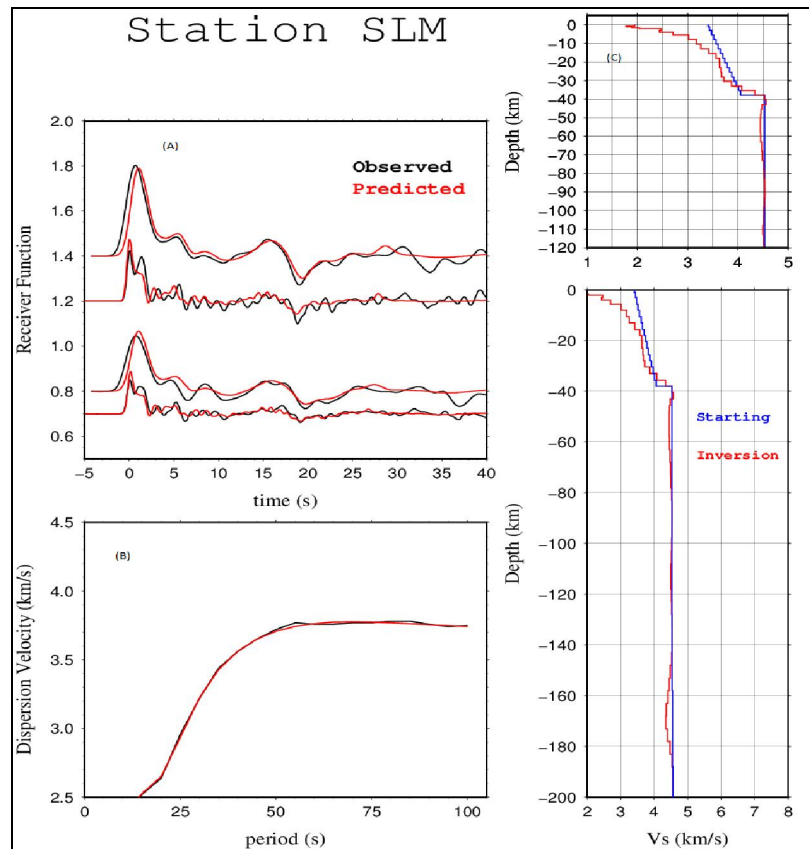


Figure 9. Results from the joint inversion for the station SLM. The three panels shown are a) Receiver functions, b) Rayleigh wave group velocities, and c) The shear wave velocity model.

Beneath the second area, the crustal thickness beneath the station SWA (Figure 7) is measured at ~ 36 km and the V_p/V_s ratio is 1.93, which consider high ratio due to the high saturated hot ground water for the very shallow subsurface. While, beneath the second station located in Frafra Oasis (FRF station, Figure 8) the crustal thickness was ~ 35 km and the average V_p/V_s ratio was 1.94, which also consider a high ratio due to the thick shallow subsurface saturated with hot ground water.

Joint inversion results

Beneath the same areas as mentioned above, we used the joint inversion of the receiver functions and the group velocity dispersion measurement to obtain the shear wave velocity models. Beneath each seismic station, an accurate velocity model is obtained by applying this joint inversion method. In fact, receiver functions are very sensitive to detect the discontinuities such as the Conrad and Moho discontinuity, while are not sensitive to the trade-off velocity (change velocity

with depths). The group velocity measurement is very sensitive to the trade-off velocity and not sensitive to the discontinuities. Therefore, a combination of these two methods, as a joint inversion will provide us with more accurate results concerning the discontinuities and the trade-off velocity.

Beneath the first area that located on the coastal line of the Mediterranean sea (SLM and DB2 stations), the shear wave velocity model was obtained, as well as a good correlation between the observed and synthetic receiver functions in addition to the observed and synthetic dispersion curves figures (9 and 10), respectively. Their velocity models are presented in tables (11 and 12).

For the second area, beneath the stations located inland, west of Egypt the joint inversion results of SWA and FRF station is shown in figures 11 and 12, respectively. The obtained velocity model beneath each station is listed in tables (13 and 14), respectively.

Table 11. Structural model beneath SLM station, V_p, V_s and density are provided.

NO.		Depth Km	P-Velocity Km/sec	S-Velocity Km/sec	Density
CRUST	surface	00	4.00	2.00	1.86
	1	5	4.70	2.70	2.3
	2	18	6.30	3.60	2.8
	3	30	6.80	4.00	2.9
MOHO		32	7.60	4.00	3.2
UPPER MANTLE		50	8.00	4.5	3.4

Table(12): Velocity model beneath DB2 station, V_p, V_s and density are provided.

NO.		Depth Km	P-Velocity Km/sec	S-Velocity Km/sec	Density
CRUST	surface	00	3.50	2.00	1.71
	1	5	5.80	3.30	2.60
	2	18	6.50	3.70	2.72
	3	30	6.80	3.90	2.94
MOHO		33	7.80	4.44	3.30
UPPER MANTLE		50	7.90	4.40	3.32

Table(13) Velocity model beneath SWA station, V_p, V_s and density are provided.

NO.		Depth Km	P-Velocity Km/sec	S-Velocity Km/sec	Density
CRUST	surface	00	3.50	2.00	1.86
	1	5	5.50	3.10	2.50
	2	18	6.20	3.50	2.75
	3	30	6.90	4.0	3.0
MOHO		36	7.80	4.40	3.25
UPPER MANTLE		50	8.00	4.50	3.30

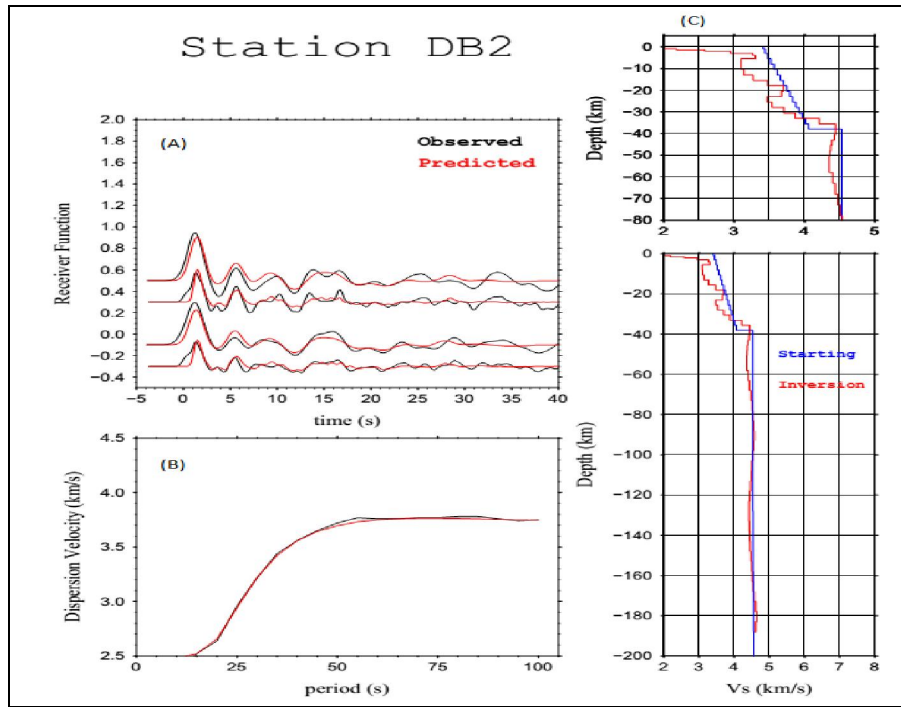


Figure (10): Results from the joint inversion for DB2 station. The three panels shown are a) Receiver function, b) Rayleigh wave group velocities and c) the shear wave velocity model.

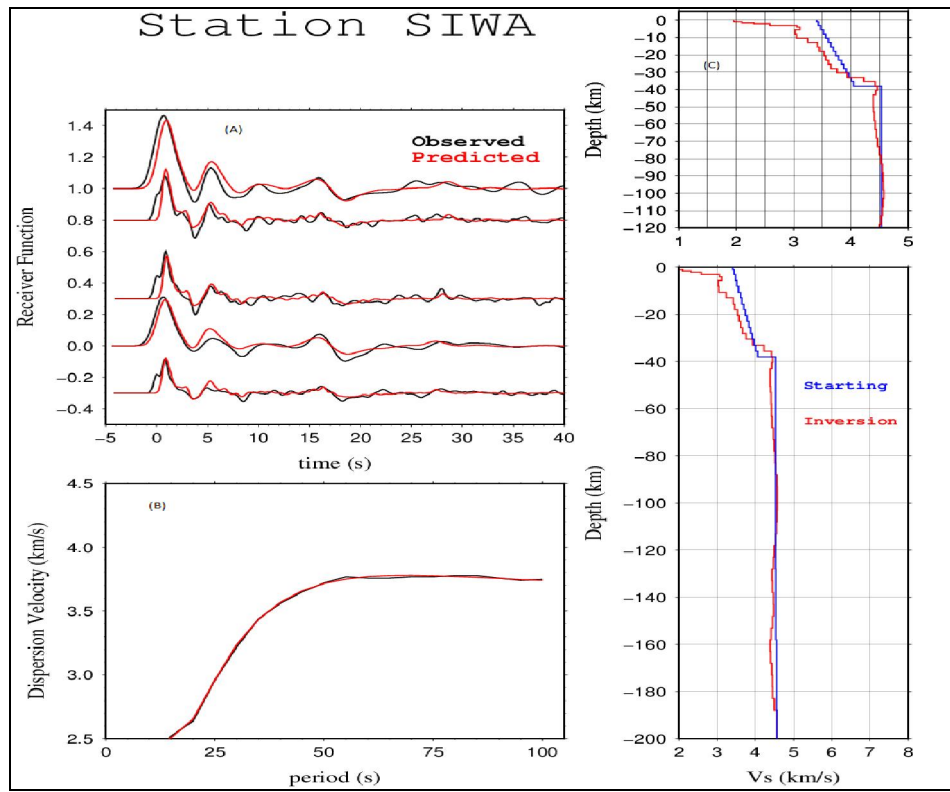


Figure (11): Results from the joint inversion tool for SWA station. The three panels shown are a) Receiver functions, b) Rayleigh wave group velocities and c) the shear wave velocity model.

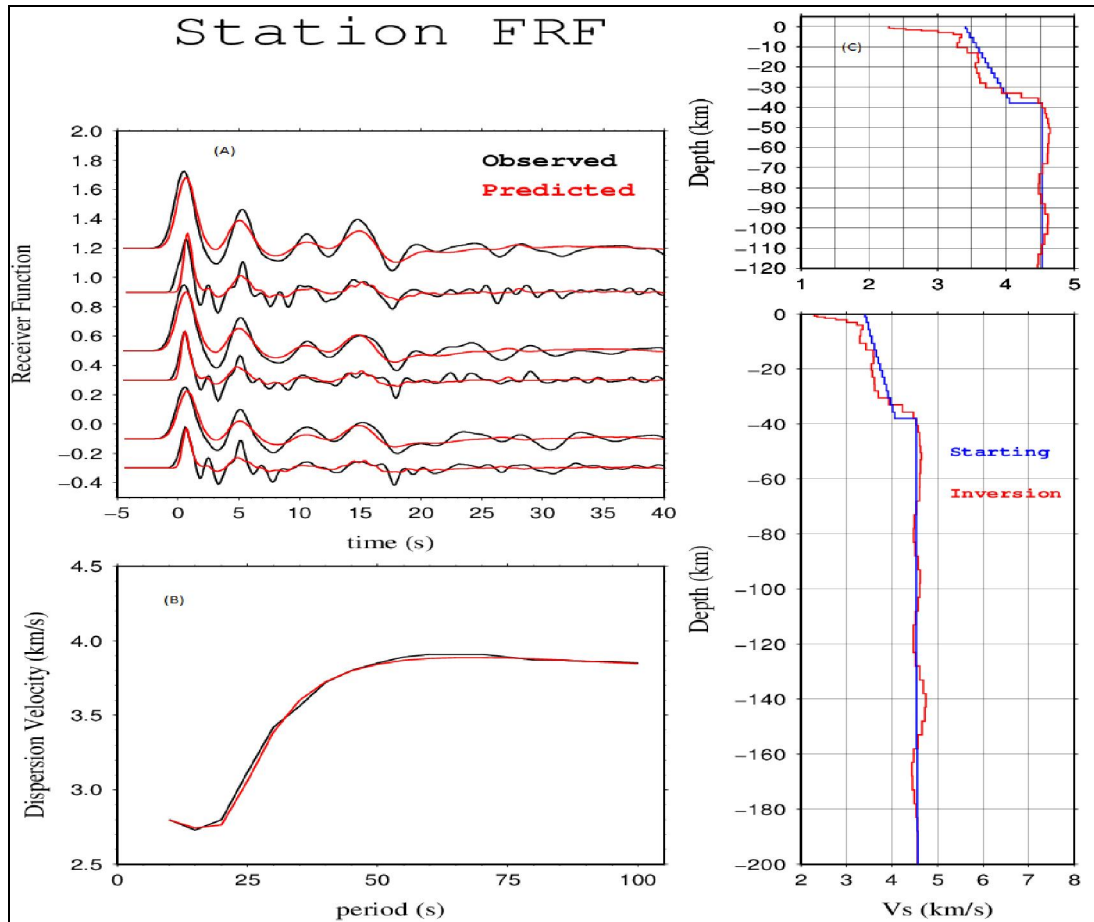


Figure (12): Results from the joint inversion for FRF station. The three panels shown are a) Receiver functions. b) Rayleigh wave group velocities, and c) The shear wave velocity model.

Table(14) Velocity model beneath the station FRF, P-wave, S-wave and density are provided.

NO.		Depth Km	P-Velocity Km/sec	S-Velocity Km/sec	Density
CRUST	superficial	00	4.20	2.40	2.10
	Middle crust	18	6.20	3.50	2.73
	Lower crust	30	6.80	3.90	3.00
MOHO		35	7.80	4.50	3.30
UPPER MANTLE		50	8.30	4.60	3.40

They showed that, the Moho discontinuity beneath the study areas is a first order boundary, where the velocity increases sharply from about 6.8 km/s (lower crust) to 8.3 km/s (Upper mantle) and the crust consists of four layers of approximately 30 km thick.

Conclusion

Basically, the crustal structure beneath the Qattara Depression has been investigated using different techniques, the transfer function, the stacking of the receiver functions, and the joint inversion of the receiver functions and the group velocity dispersions. The overall value of the crustal thickness is found to be 33 km with a standard deviation of ± 3 km. The data

with correlation coefficients less than 65% have been eliminated. The results indicate that most events showed a good correlation between the observed and the theoretical spectral ratios.

The refined results for the seismic velocity structure for the eight (BB) seismic stations around the Qattara Depression area suggested that, the crust consists of four distinct layers. The superficial layer which has a V_p of about 3.47 km/sec with thickness of about 1.56 km. The second layer has a velocity of about 5.54 km/sec and 6.14 km thick. The third layer shows a velocity of 6.26 km/sec and thickness of 16 km. The lower crustal layer has a velocity of about 6.9 km/sec and 11 km thick. The Mohorovicic

discontinuity beneath the Qattara Platform varies from 29-32 km depth in the Northern corner of Egypt and NE with 8.2 km/sec mantle velocity to 35-36 km depth in the NE and NW with 8.1 km/sec mantle velocity. The obtained model is found to be in coincidence with that obtained by Marzouk (1988).

From the above and comparing with previous crustal models The upper crust of 18 km thickness with a velocity of 6.3 km/sec. which is composed predominantly of unconsolidated sediments in the upper parts and limestone in the lower parts. The lower crust has average velocity of 7.8 km/sec and thickness of 25 km. Meissner (1986) indicated that P-wave velocities in the range 7.1-7.8 km/sec are typical of dense gabbros, eclogite, high grade granulites or mixture of crust-mantle. Crustal velocities generally increase across this boundary to the NE-SE by about 0.3 km/sec and to the SW-NW by about 0.2 km/sec

indicating either a change in the composition of basement rocks or a northwestward dip of the shield.

Based on the TF and RFs results, the average crustal thickness beneath the study area ranges from 32-35 km with an average Vp/Vs ratio of 1.9, which consider a high value. In fact this area is characterized by thick soft sediments saturated with hot water, therefore a high value of Vp/Vs ratio is observed.

The shear wave velocity models obtained from the joint inversion revealed the Moho depths beneath each seismic station, which consists with the results obtained by stacking the RFs.

For the study area, using results obtained from TF and RFs an average velocity model is provided, as listed in table (15). This average velocity model will be utilized for locating local and regional earthquakes occur in and around the Qattara area and even for the north Egypt part.

Table (15). An average velocity model for the study area.

NO.		Depth Km	P-Velocity Km/sec	S-Velocity Km/sec	Density
CRUST	superficial	00	4.30	1.93	1.85
	Middle crust	18	6.54	3.30	2.53
	Lower crust	30	6.90	3.94	3.00
MOHO		35	7.75	4.40	3.30
UPPER MANTLE		50	8.10	4.55	3.33

Acknowledgements

This research study is supported by the Science Technology and Development Fund, Egypt (STDF), under the project number 5314. We also appreciate and thank the Egyptian National Seismic Network Laboratory (ENSN), seismology department, at the National Research Institute of Astronomy and Geophysics (NRIAG) for providing the seismic data needed for implementing the proposed study.

References

1. Al Amri A., and Gharib A. A., 2000. Lithosphere seismic structure of the eastern region of Arabian Peninsula. *Journal of Geodynamics*, V. 29, P. 125-139.
2. Ammon C. J. and G. Zandt (1990): Receiver structure beneath the southern Mojave block, California, *Bull. Seism. Soc. Am.*, 83, 737-755.
3. Gharib, A. A., 2005, Estimation of the crustal structure beneath the Kottamia region –Egypt using P-wave spectral ratios of vertical to horizontal component. 4th International symposium on geophysics, Tanta (2006), p. 92-103.
4. Haskell, N.A. (1953). The dispersion of surface waves in multilayered media, *Bull. Seism. Soc. Am.* 43, 17-34.
5. Haskell, N.A., 1962, Crustal reflection of plane P and SV- waves, *J. Geophys. Res.*, v. 69, p. 1797-1809.
6. Hegazi, M., 2007: Constructing A Velocity Crustal Structural Model Using P-wave Spectral Ratios Beneath The Seismic Stations In The North Of Egypt. Master Thesis. Ain Shams University.
7. Dugda, M. T., Nyblade, A. A., J. Julià, (2007). Thin lithosphere beneath 831 the Ethiopian Plateau revealed by a joint inversion of Rayleigh wave group velocity and receiver functions, *J. Geophys. Res.*, 112, B08305, doi:10.1029/2006JB004918.
8. Fernandez. L M., 1965, The determination of crustal thickness from the spectrum of P waves. Scientific report. No 13, St. Louis University, Missouri, USA.
9. Gharib A. A., 2006. Estimation of the crustal structure model beneath the Kottamia region-Egypt using P-wave spectral ratios of vertical to horizontal component. 4th International symposium on geophysics, Tanta (2006), P. 92-103.
10. Gharib A. A., 2006. Crustal structure of Tushka region, Abu-Simbel, Egypt, inferred from spectral ratios of P waves of local earthquakes *Acta. Geophysica*, vol., 54, no.4, pp.361-377. DOI:10.2478/s11600-006-0026-7.

11. Juli, J., C.J. Ammon, R.B. Herrmann, and A.M. Correig (2000) Joint inversion of receiver function and surface wave dispersion observations, *Geophys. J. Int.*, 143, 1-19.
12. Julià, J., Ammon, C. J., Herrmann, R. B., (2003). Lithosphere structure of the Arabian Shield from the joint inversion of receiver functions and surface-wave group velocities. *Tectonophysics*. 825-837, 1-21.
13. Julià, J., C. J. Ammon, and Nyblade, A. A., (2005). Evidence for mafic lower crust in Tanzania, East Africa, from joint inversion of receiver functions and Rayleigh wave dispersion velocities, *Geophys. J. Int.*, 162, 255-569.
14. Langston, C.A., (1979) Structure under Mount Rainier, Washington, inferred from teleseismic body waves: *J. Geophys. Res.*, 85, 4749-4762.
15. Ligorra, J. P. and C. J. Ammon (1999) Iterative deconvolution and receiver function estimation, *Bull. Seism. Soc. Am.*, 89, 1395-1400.
16. Maamoun, M., 1979: Macroseismic Observations of principal Earthquakes in Egypt. HIAG, Bulletin No. 183, Helwan, 1979.
17. Marzouk, I., 1988, Study of crustal structure of Egypt deduced from deep seismic sounding and gravity data. Homburg University, Germany.
18. Meissner (1986). The continental crust, A geophysical Approach, International Geophysical Series, v., 34. San Diego, Academic Press, p., 462.
19. Ozalaybey, S., M. K. Savage, A. F. Sheehan, J. N. Louie, and J. N. Brune (1997), Shear-wave velocity structure in the northern Basin and Range province from the combined analysis of receiver functions and surface waves, *Bulletin of the Seismological Society of America*, 87, 183-199.
20. Phinney, R. A., 1964, Structure of the earth's crust from spectral behavior of long-period body waves. *J. Geophys. Res.*, v. 69, p. 2997-3017.
21. SOFRATOME Group, 1984, El-Dabaa Nuclear Power Plant, unpublished report, Ministry of Energy and Electricity, Egypt.
22. Sestini, G., 1989, Nile Delta: A review of depositional environmental and geological history, *Deltas: sites and Traps for fossil fuels*. Geological Society Special Publication. No 41, pp 99-127.
23. Thomson, W.T. 1950, Transmission of elastic waves through a stratified solid medium. *J. App. Phys.*, v. 21, p. 89-93.
24. Zandt, G. and C. J. Ammon (1995) Continental crust composition constrained by measurements of crustal Poisson's ratio, *Nature*, 374, 152-155.
25. Zhu, L. and Kanamori, H. (2000). Moho depth variation in Southern California from teleseismic receiver functions, *Journal of Geophysical Research*, 105, 2969-2980.

2/28/2016